

# ***In vivo* native fluorescence spectroscopy and nicotinamide adenine dinucleotide/flavin adenine dinucleotide reduction and oxidation states of oral submucous fibrosis for chemopreventive drug monitoring**

**Shanmugam Sivabalan**

Anna University Chennai  
Department of Physics  
Division of Medical Physics and Lasers  
Chennai, 600 025 India

**C. Ponranjini Vedeswari  
Sadaksharam Jayachandran**

Tamilnadu Government Dental College and Hospital  
Department of Oral Medicine and Radiology  
Chennai, 600 003 India

**Dornadula Koteeswaran  
Chidambaranathan Pravda**

Meenakshi Ammal Dental College and Hospital  
Department of Oral Medicine and Radiology  
Chennai, 600 095 India

**Prakasa Rao Aruna  
Singaravelu Ganesan**

Anna University Chennai  
Department of Physics  
Division of Medical Physics and Lasers  
Chennai, 600 025 India

**Abstract.** Native fluorescence spectroscopy has shown potential to characterize and diagnose oral malignancy. We aim at extending the native fluorescence spectroscopy technique to characterize normal and oral submucous fibrosis (OSF) patients under pre- and post-treated conditions, and verify whether this method could also be considered in the monitoring of therapeutic prognosis noninvasively. In this study, 28 normal subjects and 28 clinically proven cases of OSF in the age group of 20 to 40 years are diagnosed using native fluorescence spectroscopy. The OSF patients are given dexamethasone sodium phosphate and hyaluronidase twice a week for 6 weeks, and the therapeutic response is monitored using fluorescence spectroscopy. The fluorescence emission spectra of normal and OSF cases of both pre- and post-treated conditions are recorded in the wavelength region of 350 to 600 nm at an excitation wavelength of 330 nm. The statistical significance is verified using discriminant analysis. The oxidation-reduction ratio of the tissue is also calculated using the fluorescence emission intensities of flavin adenine dinucleotide and nicotinamide adenine dinucleotide at 530 and 440 nm, respectively, and they are compared with conventional physical clinical examinations. This study suggests that native fluorescence spectroscopy could also be extended to OSF diagnosis and therapeutic prognosis. © 2010 Society of Photo-Optical Instrumentation Engineers. [DOI: 10.1117/1.3324771]

**Keywords:** autofluorescence; fluorescence spectroscopy; collagen; oral submucous fibrosis; intrinsic fluorophores; chemopreventive; discrimination analysis; optical spectroscopy.

Paper 09185RR received May 10, 2009; revised manuscript received Jan. 3, 2010; accepted for publication Jan. 5, 2010; published online Mar. 2, 2010.

## **1 Introduction**

Head and neck cancer is one of the most common cancers in the world, nearly two-thirds of which occur in developing countries. The overall survival rates for cancer are low in developing countries.<sup>1</sup> It is well documented that most invasive oral cancers arise from precancerous lesions such as leukoplakia, erythroplakia, and oral submucous fibrosis (OSF).<sup>2</sup> OSF is a high-risk precancerous condition with a reported prevalence ranging up to 0.4% in Indian rural populations.<sup>3</sup> The histopathological feature of OSF includes atrophy of oral epithelium with parakeratosis or hyperkeratosis, as well as marked collagen deposition and hyalinization in the lamina propria, submucous, and superficial muscle layer.<sup>4</sup> Many reported that the chewing of areca nut and tobacco is a major possible cause for OSF in India, which includes genetic, viral, autoimmune, and carcinogenic agents.<sup>5,6</sup>

Although the accessibility of the oral cavity is easier than other sites, most patients present with advanced stages and require more aggressive treatment. This result yields very poor survival rate and higher morbidity,<sup>7</sup> and hence there arises a need for early detection techniques. However, conventional screening and detection of oral cancer by visual inspection of the oral cavity with white light may be difficult to discriminate the early stage or oral cancer from nonspecific inflammation and irritation.<sup>8</sup> In this regard, various optical spectroscopic techniques, such as fluorescence spectroscopy,<sup>9,10</sup> diffuse reflectance spectroscopy,<sup>11,12</sup> synchronous luminescence spectroscopy,<sup>13</sup> and Raman spectroscopy,<sup>14</sup> have been considered to characterize and diagnose oral neoplasia and imaging. Among various optical spectroscopic techniques, native fluorescence spectroscopy has been widely considered in the characterization of metabolic and pathological conditions of cells and tissues at the molecular level due to its sensitivity and availability of many complementary techniques.

---

Address all corresponding to: Singaravelu Ganesan, Professor, Division of Medical Physics and Lasers, Department Of Physics, Anna University Chennai, Chennai 600 025, India. Tel: 91-44-22358685; Fax: 91-44-222352270; Email: sganesan@annauniv.edu

Using native fluorescence spectroscopy, different pathological conditions of oral malignancies were better discriminated from normal subjects with very high statistical significance.<sup>15-17</sup> Among various native fluorophores present in oral tissues, the emission contribution from tryptophan, collagen, flavin adenine dinucleotide (FAD) and nicotinamide adenine dinucleotide (NADH), and endogenous porphyrins were exploited in the discrimination of normal from oral malignancies. The fluorescence of collagen, elastin, and more generally proteins is due to the presence of aromatic amino acids that relate to the structural arrangement of cells and tissue. NADH, FAD, and endogenous porphyrin are related to metabolic processes or are in connection with the onset of pathological conditions.<sup>18-20</sup> Further, it is also reported that the emission characteristics of these native fluorophores also vary with different anatomical sites of the oral cavity.<sup>21,22</sup> Recently, the relative change in the fluorescence emission intensity of FAD and NADH was also considered to study the oxidation-reduction state of cells, as the redox ratio is used to monitor the cellular metabolic rate under normal and neoplastic conditions.<sup>23,24</sup>

Although many extensive studies were made in the characterization and diagnosis of cancer using native fluorescence spectroscopy, to the best of our knowledge there are no reports of *in vivo* study on the monitoring of treatment prognosis of OSF. In this context, the focus of the study was on the *in vivo* characterization of healthy and OSF patients under pre- and post-treated conditions using native fluorescence spectroscopy. Attempts were also made to verify the statistical significance of the prior techniques in the discrimination of normal from OSF as well as pretreated OSF conditions from post-treated conditions.

## 2 Materials and Methods

### 2.1 Patients

28 patients having a premalignant lesion condition of OSF from the Tamilnadu Government Dental College and Hospital Chennai, India, but not having any systemic diseases such as diabetes, hypertension, hepatic or renal diseases, or patients with any kind of allergy, were involved in this study. All patients had a chewing habit for more than three years and patients with grade IV and V oral submucous fibrosis were involved in this study. All patients had a mouth opening greater than 15 mm and an intolerance to spicy food, with fibrous bands in buccal mucosa. The clinical diagnoses were confirmed with the histopathological reports.

28 healthy volunteers with no clinically observable lesion and no habit of chewing areca (betel) nut or tobacco were used as normal subjects. All the patients and volunteers were in the age group of 20 to 40 years.

### 2.2 Oral Submucous Fibrosis Treatment

Patients were given an intralesional injection of a combination of dexamethasone sodium phosphate (4 mg/ml) and hyaluronidase (1500 IU) twice a week for 6 weeks. They were also given antioxidants and micronutrient supplementation and were taught muscle stretching exercises. All the treatments were implemented at the Tamilnadu Government Dental College and Hospital, Chennai, India.

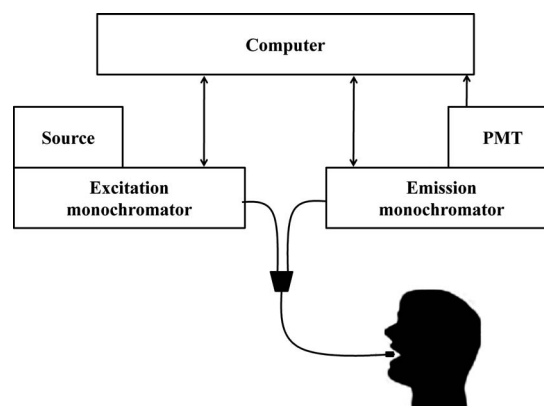


Fig. 1 Schematic diagram showing the *in vivo* fluorescence measurement setup.

Dexamethasone sodium phosphate injection (4 mg/ml) marketed by Prem Pharmaceuticals (Bangalore, India) was used in the study. Each milliliter of solution contains dexamethasone sodium phosphate IP equivalent to dexamethasone phosphate 4 mg, and methylparaben IP 0.18% w/v and propylparaben IP 0.02% w/v as preservatives.

Hyaluronidase injection used in the study was hyaluronidase IP, manufactured by Shreya Life Sciences (Aurangabad, India). Each vial contains hyaluronidase as a freeze-dried powder, providing activity equivalent to 1500 IU.

At each visit, following the topical application of lignocaine 2%, 1500 IU of hyaluronidase was dissolved in 2.0 ml of dexamethasone sodium phosphate in a 2-ml disposable syringe. The drugs were injected at multiple sites where the fibrotic bands were palpable submucosally by means of a gauge 24 needle, not more than 0.2-ml solution per site.

The patients were clinically examined at every visit during the treatment period of 6 weeks by evaluating maximal mouth opening (MMO) and tongue protrusion (TP).

### 2.3 Steady-State Fluorescence Measurements

The *in vivo* fluorescence was recorded using a Fluoromax-2 (ISA Jobin Yvon-Spex, Edison, New Jersey) spectrofluorometer. The excitation source (150-W ozone-free xenon arc lamp) coupled to the monochromator delivers light to the sample spot at a desired wavelength, and the fluorescence emission from the tissues is collected by another monochromator connected to a photomultiplier tube (R928P, Hamamatsu, Shizuoka-Ken, Japan). The gratings in the excitation and emission monochromators have a groove density of 1200 grooves/mm and are blazed at 330 and 500 nm, respectively. During fluorescence data acquisition, the excitation and emission slit widths are set at 5 and 8 nm, respectively, with an integration time of 0.5 s. The collected signal is transferred to a PC through an RS232 interface. The data were processed by the Windows-based data acquisition program Data Max powered by GRAMS/386. In the *in vivo* measurements, a bifurcated randomized fiber optic bundle of model 1950M is used with the fiber optic platform of model 1950F (see Fig. 1).

During fluorescence measurements, the common end of the fiber assembly is kept perpendicular to the tissue surface,

whereas the excitation and collection ends of the fiber assembly are connected to the excitation and emission monochromators, respectively. As the fluorescence emission from the tissues is highly anisotropic and they are emitted in all directions, more fibers are used at the collection end of the fiber assembly to improve collection efficiency. Further, to collect the maximum fluorescence signal over the solid angle of its emission, the common end of the fiber assembly is designed such that there is always a distance of 3 mm between the tissue surface and the fiber tip during the measurements. Before recording the spectra, all the volunteers and OSF patients were asked to rinse their mouth for 1 min with saline solution to eliminate the influence of consumed food. The probe is placed at the site where fibrotic bands are palpable, as suggested by the physician, and for each site two spectra were recorded.

#### 2.4 Reduction and Oxidation Ratio

The reduction and oxidation ratio was computed using the relation

$$\text{redox ratio} = \frac{\text{FAD}_{\text{intensity}}}{\text{FAD}_{\text{intensity}} + \text{NADH}_{\text{intensity}}},$$

where FAD intensity and NADH intensity are the emission intensity of FAD and NADH at 530 and 440 nm, respectively.<sup>25</sup>

#### 2.5 Data Processing

**Normalization.** Each fluorescence spectrum was normalized by dividing the fluorescence intensity at each emission wavelength by the peak emission intensity of the spectrum. Normalizing a fluorescence spectrum removes absolute intensity information, and the main advantage of utilizing a normalized spectrum is that fluorescence intensity does not need to be recorded in calibrated units.<sup>26,27</sup>

**Introducing ratio variables.** To quantify the results and to estimate the potential of the present technique, 12 ratio variables were introduced. Emission wavelengths  $390 \pm 10$ ,  $450 \pm 10$ , and  $530 \pm 10$  nm were taken by considering the peak emission wavelength of collagen, NADH, and FAD, respectively. The mean and standard error values of all the ratio variables were calculated for each group of experimental subjects. A two-tailed student's t-test was performed to determine the level of significance ( $p$  value) with which each ratio variable discriminates diseased subjects with respect to normal subjects.

The following three different discriminant analysis were performed to:

1. discriminate between the OSF patients and the normal subjects ( $D_1$ )
2. discriminate between pre- and post-treated OSF conditions ( $D_2$ )
3. find the discrimination factor for normal, pre-, and post-treated conditions ( $D_3$ )

In the present work, the discriminant analysis was performed using SPSS (SPSS Incorporated, Chicago, Illinois). This analysis used a partial F-test (F to enter 3.84 and F to remove 2.71) and a step-wise method to sequentially incorpo-

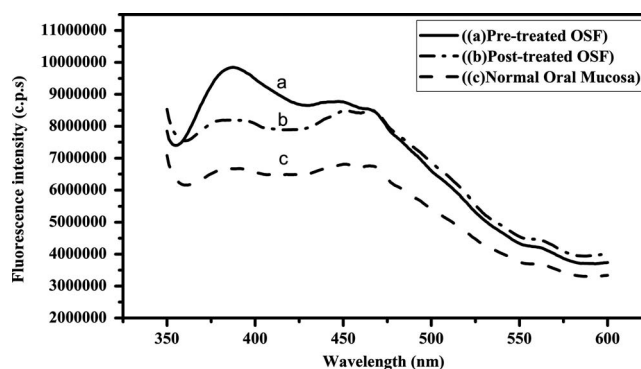


**Fig. 2** *In vivo* fluorescence spectra of normal (---), pretreated (—), and posttreated (—●—) OSF cases and normal in the wavelength region 350 to 650 nm at an excitation of 330 nm. The spectra were measured at every 1-nm interval with an integration time of 0.5 sec. The excitation and emission slit widths were kept at 5 and 8 nm, respectively.

rate the set of 12 variables into a Fisher linear discriminant function. Step-wise analysis based on maximizing an F ratio was computed from the Mahalanobis distance (measure of how much a case's values on the independent variables differ from the average of all cases. A large Mahalanobis distance identifies a case as having extreme values on one or more of the independent variables) between the groups. Further, we use leave-one-out cross-validation. In this procedure, discriminant scores of one particular sample were eliminated, and discriminant analysis was used to form a classification algorithm using the remaining samples. The resulting algorithm was then used to classify the excluded case. This process was repeated for each sample.

### 3 Results

The native fluorescence emission spectra from healthy oral mucosa, OSF under both pre- and post-treated conditions, were measured at 330-nm excitation ( $\lambda_{\text{em}}=350$  to 600 nm). The individual case and clinical details of OSF patients such as age, duration, and frequency per day of areca net chewing, clinical grading, MMO, and TP before and after treatment are given in Table 1.

#### 3.1 *In Vivo* Fluorescence Spectroscopy

The averaged fluorescence emission spectra of healthy subjects and patients with OSF under pre- and post-treated conditions at 330-nm excitation are shown in Fig. 2. The fluorescence emission spectra of normal and OSF (under pre- and post-treated) show two peaks centered at 390 and 465 nm, with a well in-between the two peaks at 420 nm. The emission intensity at 390 nm for OSF cases is higher than that of the emission at 465 nm. On the other hand, the emission peak at 390 nm for normal oral mucosa is considerably less than that at 460 nm. The overall fluorescence intensity of OSF cases is higher than that of normal subjects. Further, it is observed that the emission intensity of OSF at 390 nm is around 1.25 times higher than that of normal mucosa. The fluorescence emission spectra of OSF patients were also measured after a 7-week period of the post-treatment as discussed in Sec. 2. The fluorescence emission spectra of post-treated

**Table 1** Clinical report of the individuals before and after treatment who were involved in the study (BT is before treatment and AT is after treatment).

Number	Age/ Sex	Areca quid chewing		Duration of symptoms (in months)	Sites of involvement	Clinical grading	Maximal mouth opening (in mm)		Tongue protrusion (in mm)	
		Duration in months	Frequency per day				BT	AT	BT	AT
1	38/F	276	2	60	4	V	17	26	15	20
2	26/M	180	15	6	4	IV	22	30	30	30
3	20/M	180	10	3	6	V	16	28	15	25
4	40/M	240	12	24	6	IV	17	32	30	35
5	27/M	120	10	36	5	IV	19	29	30	30
6	26/M	360	15	3	5	V	20	32	20	25
7	36/M	600	6	12	4	V	16	28	20	30
8	29/M	240	3	12	4	IV	18	31	30	30
9	20/M	120	4	3	6	IV	20	31	30	25
10	28/M	240	3	1	4	V	20	32	15	20
11	40/F	120	3	8	5	V	16	29	15	30
12	38/M	180	8	12	5	V	19	30	15	25
13	35/M	120	25	3	4	IV	17	28	30	30
14	36/M	300	5	12	3	IV	16	29	25	30
15	40/M	240	2	12	6	IV	18	29	25	25
16	40/M	120	3	12	5	V	21	31	10	25
17	38/M	600	6	18	4	IV	16	26	25	35
18	30/M	720	5	4	4	V	16	24	20	25
19	39/M	960	5	12	3	V	18	30	15	20
20	24/M	240	5	18	3	IV	20	31	30	30
21	28/F	220	10	15	5	V	16	28	15	25
22	37/M	200	15	12	6	V	17	32	30	35
23	42/M	280	4	10	8	V	17	31	15	25
24	30/M	320	2	18	4	IV	15	26	25	35
25	21/M	600	12	6	4	IV	16	30	15	30
26	27/M	720	2	12	3	IV	19	30	15	25
27	39/F	960	3	18	6	V	19	26	15	20
28	40/M	320	7	8	5	V	22	32	30	32

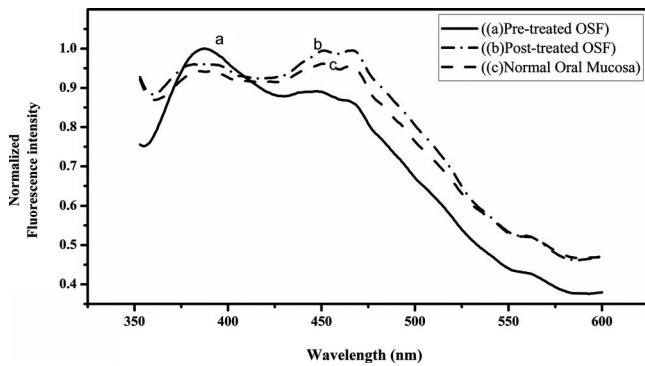


**Fig. 3** Averaged normalized *in vivo* fluorescence spectra of pretreated (—) and post-treated (—●—) OSF cases and normal (- - -) in the wavelength region 350 to 650 nm at an excitation of 330 nm. The spectra were measured at every 1 nm interval with an integration time of 0.5 sec. The excitation and emission slit widths were kept at 5 and 8 nm, respectively.

OSF cases have spectral signatures similar to that of normal oral mucosa, i.e., the emission intensity at 390 nm is less than that at 465 nm. However, it is noted that the overall fluorescence intensity is comparatively less than that of the normal subjects.

Figure 3 shows the averaged normalized emission spectra of normal, pre-treated, and post-treated OSF cases. From Fig. 3, it is clearly observed that the emission intensity at 390 nm for normal and post-treated OSF cases is less than that at 465 nm. Both the normal and post-treated cases exhibit similar spectral signatures.

### 3.2 Statistical Analysis

To quantify and verify the statistical significance of the observed spectral differences between normal and OSF patients, as well as the spectral differences between pre- and post-treated OSF patients, 12 statistically significant ratio variables were introduced. The mean values of these ratio variables with standard deviation for the previous groups are given in Table 2. In comparison of normal and pretreated OSF cases, the  $P$  value for most of the ratio parameters is highly significant ( $p=0.001$ ), except for the variables  $V_{11}$  and  $V_{12}$ , whose  $p$  values are found to be 0.1. Similarly, in comparison of pretreated cases with post-treated OSF cases, the ratio variables are highly significant, with  $p$  value less than 0.0001. From this, it is observed that all the ratio values of normal and post-treated conditions of OSF are almost the same, and they differ from pretreated OSF cases with excellent statistical significance. The ratio variables included for discriminant analysis are given in Table 2.

These ratio variables were subjected to the step-wise multiple linear discriminant analysis as follows.

#### 3.2.1 Discriminant Analysis 1 (Discrimination of Oral Submucous Filorosis from Normal)

The step-wise multiple linear discriminant analysis was performed between the 28 pretreated and 28 normal subjects, resulting in the following expression for a canonical discriminant function (DF):

$$D_1 = 8.946(V_1) - 26.464(V_5) - 3.891(V_7) + 26.253(V_{11}) - 1.641.$$

**Table 2** The ratio parameters used for statistical analysis with mean $\pm$ SD after passing the student t-test.

Variables	Parameters	Normal	Pretreated	Post-treated
$V_1$	$I_{385}/I_{550}$	1.869 $\pm$ 0.053	2.377 $\pm$ 0.115	1.778 $\pm$ 0.048
$V_2$	$I_{387}/I_{550}$	1.868 $\pm$ 0.053	2.382 $\pm$ 0.116	1.778 $\pm$ 0.049
$V_3$	$I_{390}/I_{550}$	1.868 $\pm$ 0.053	2.379 $\pm$ 0.116	1.789 $\pm$ 0.050
$V_4$	$I_{385}/I_{468}$	0.959 $\pm$ 0.010	1.161 $\pm$ 0.024	0.915 $\pm$ 0.022
$V_5$	$I_{387}/I_{468}$	0.958 $\pm$ 0.009	1.164 $\pm$ 0.024	0.915 $\pm$ 0.022
$V_6$	$I_{390}/I_{468}$	0.958 $\pm$ 0.009	1.162 $\pm$ 0.024	0.919 $\pm$ 0.021
$V_7$	$I_{385}/I_{335}$	1.091 $\pm$ 0.022	1.375 $\pm$ 0.057	1.075 $\pm$ 0.038
$V_8$	$I_{387}/I_{355}$	1.090 $\pm$ 0.022	1.379 $\pm$ 0.058	1.076 $\pm$ 0.039
$V_9$	$I_{390}/I_{355}$	1.090 $\pm$ 0.022	1.377 $\pm$ 0.059	1.083 $\pm$ 0.040
$V_{10}$	$I_{387}/I_{430}$	1.025 $\pm$ 0.009	1.132 $\pm$ 0.014	0.962 $\pm$ 0.018
$V_{11}$	$I_{530}/I_{450}$	0.602 $\pm$ 0.011	0.572 $\pm$ 0.014	0.601 $\pm$ 0.013
$V_{12}$	$I_{450}/I_{530}$	1.676 $\pm$ 0.033	1.779 $\pm$ 0.046	1.685 $\pm$ 0.038

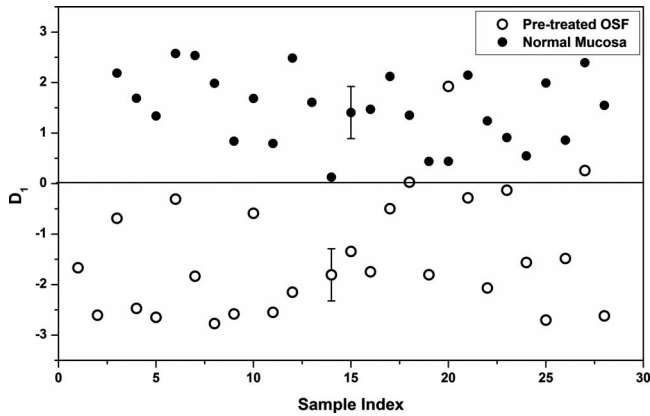


**Fig. 4** Scatter plot showing the distribution of  $D_1$  for normal (●) and pretreated (○) oral submucous fibrosis.

Of these 12 input variables, four variables turned out to be significant and were included in the linear discriminant function. Figure 4 shows the scatter plot of the discriminant score, i.e., the value of the discriminant function for normal and OSF individuals.  $D_1$  shows that OSF cases are discriminated

with a sensitivity of 89% using the present techniques. In this discriminant analysis, out of 28 OSF cases, three cases were misclassified as normal. However, all the normal groups were classified correctly with a specificity of 100%. In this analysis, it is also obtained that 95% of the original grouped cases and 93% of the cross-validated grouped cases were correctly classified. From the figure it is observed that the value of  $D_1$  is greater than zero for normal oral mucosa, and  $D_1$  is less than zero for pretreated conditions (Fig. 4). The classification results of this discriminant analysis are given in Table 3.

**3.2.2 Discriminant Analysis 2 (Discrimination of Pretreated Oral Submucous Fibrosis from Post-Treated Oral Submucous Fibrosis)**

The step-wise multiple linear discriminant analysis was also performed across the whole set of 28 pre- and post-treated OSF cases, resulting in the following expression for a canonical discrimination function:

$$D_2 = 8.308(V_4) - 8.626.$$

Of these 12 variables, only one variable turned out to be significant. From these 12 input variables,  $V_4$  ( $I_{385}/I_{460}$ )

**Table 3** Classification results of the discriminant analysis done across the different groups. Bold values represent the specificity/sensitivity value of the corresponding groups. The total percentage of correctly classified cases gives the average of the percentage of predicted groups.

Discriminant analysis	Cases	Group	Percentage of predicted group			Total percentage of correctly classified cases
			1	2	3	
$D_1$	Original	1.00	<b>89.3</b>	10.7	—	94.6
		2.00	0.0	<b>100.0</b>	—	
	Cross-validated	1.00	<b>89.3</b>	10.7	—	92.9
		2.00	3.6	<b>96.4</b>	—	
$D_2$	Original	1.00	<b>85.7</b>	14.3	—	89.3
		2.00	7.1	<b>92.9</b>	—	
	Cross-validated	1.00	<b>85.7</b>	14.3	—	89.3
		2.00	7.1	<b>92.9</b>	—	
$D_3$	Original	1.00	<b>71.4</b>	25.0	3.6	69.0
		2.00	0.0	<b>71.4</b>	28.6	
		3.00	7.1	28.6	<b>64.3</b>	
	Cross-validated	1.00	<b>71.4</b>	25.0	3.6	69.0
		2.00	0.0	<b>71.4</b>	28.6	
		3.00	7.1	28.6	<b>64.3</b>	

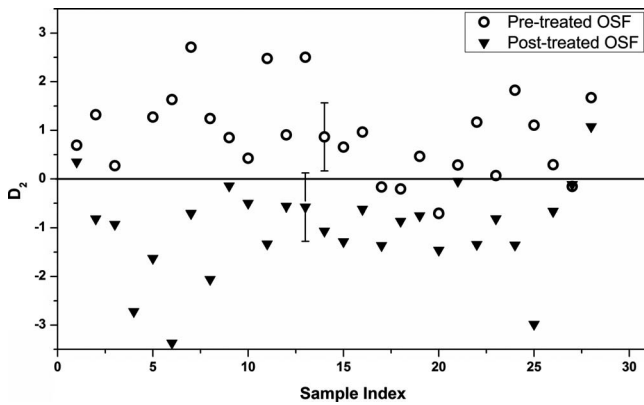


Fig. 5 Scatter plot showing the distribution of  $D_2$  for pretreated (○) and post-treated (▼) oral submucous fibrosis.

turned out to be significant and was included in the linear discriminant function  $D_2$ . Figure 5 shows the scatter plot of the discriminant score, i.e., the values of discriminant function for pre- and post-treated OSF patients. In this analysis, the pre- and post-treated conditions are correctly classified with 86 and 93%, respectively. From the scattered plot, it is observed that  $D_2$  is greater than zero for pretreated cases, and  $D_2$  is less than zero for post-treated cases.

### 3.2.3 Discriminant Analysis 3

A third discriminant analysis was carried out across normal, pretreated OSF and post-treated OSF groups. Among 12 variables, only four variables— $V_2$ ,  $V_6$ ,  $V_8$ , and  $V_{12}$ —were retained in this analysis. Resulting canonical discriminant functions are given by

$$D_{3a} = 263.934(V_2) - 390.631(V_6) + 10.59(V_8) + 1499.009(V_{12}) - 522.763,$$

$$D_{3b} = 291.072(V_2) - 470.908(V_6) - 1.214(V_8) + 1578.650(V_{12}) - 527.741.$$

Figure 6 shows the scatter plot of  $D_{3a}$  versus  $D_{3b}$ , the

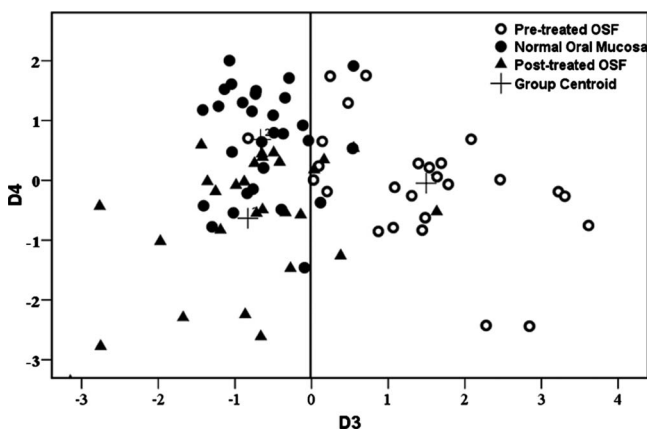


Fig. 6 Scatter plot showing the distribution of  $D_3$  versus  $D_4$  for normal, pretreated, and post-treated oral submucous fibrosis.

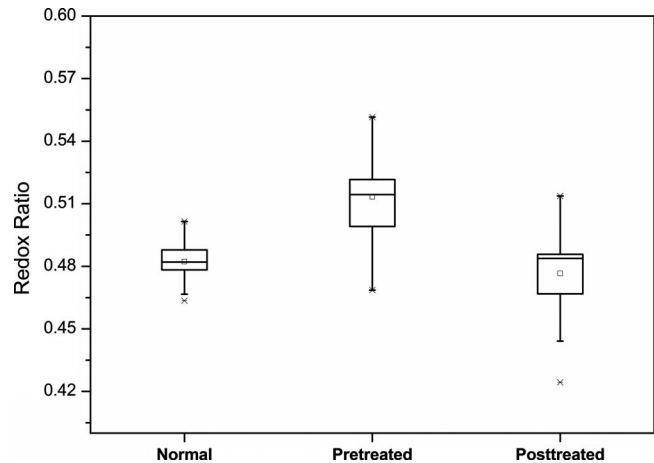


Fig. 7 *In vivo* optical redox ratio [Fluorescence intensity of FAD/(NADH+FAD)] for the normal, pretreated, and post-treated oral submucous fibrosis. Box plot includes the mean, standard error, and standard deviation.

corresponding group centroids and the standard deviation from the group centroids. The classification results are shown in Table 3. From  $D_3$  analysis, pre- and post-treated OSF, and normal mucosa were compared, and it was found that all the pretreated OSF cases showed values of  $D_{3a}$ , which is greater than zero, and the normal and post-treated OSF showed  $D_{3a}$ , which is less than zero (Fig. 6). Further, it was found that the discriminant factor  $D_3$  for normal and post-treated cases grouped together, and they were well discriminated from the pretreated OSF cases. This clearly indicates that there is a significant change in the oral cavity due to treatment.

### 3.3 Reduction and Oxidation Ratio

The metabolic coenzymes FAD and NADH are considered to be the primary electron acceptor and donor, respectively, in oxidative phosphorylation. Cellular metabolism is also associated with the change in relative concentration of these fluorophores to both be under free and bound conditions with other proteins. Also, these changes considerably differ for abnormal cells when compared to that of their normal counterparts. As these metabolic coenzymes (FAD and NADH) are highly fluorescent molecules, the relative change in the oxidation-reduction state (redox) of the cell is monitored non-invasively using optical techniques. The most common method of measuring this redox state of the cells is the computation of the ratio of fluorescence intensity of FAD and NADH, as this ratio is considered to be sensitive to cellular metabolism as well as vascular oxygen supply. The computed values of redox potentials for normal, pretreated, and post-treated OSF groups are shown in Fig. 7. From Fig. 7, it is clearly observed that the redox ratio value of pretreated OSF cases is considerably higher than that of normal subjects and post-treated cases.

### 3.4 Measurements of Maximal Mouth Opening and Tongue Protrusion

The MMO and TP were also measured for both pre- and post-treated OSF cases. Table 1 shows the measured values of the same for individual cases under both pre- and post-treated

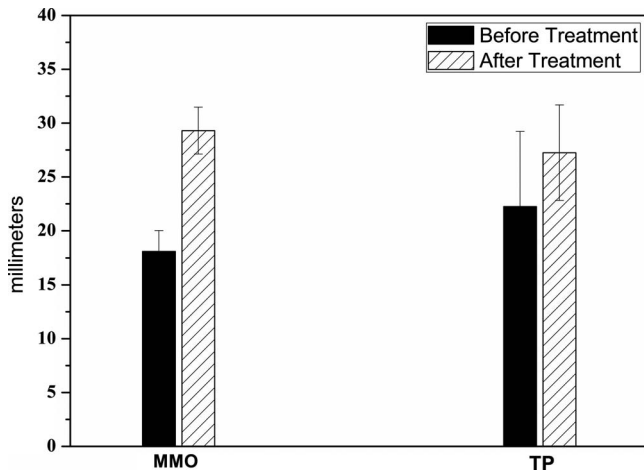


**Fig. 8** Clinical evaluation of the patients (mamimum mouth opening and tongue protrusion) before and after treatment to monitor the treatment prognosis.

conditions. Figure 8 shows the overall change in the value MMO and TP for pre- and post-treated cases. From Fig. 9, it is observed that both clinical evaluations show considerable differences between pre- and post-treated OSF cases. The variations are 38 and 20% in the MMO and TP values, respectively, for post-treated conditions with respect to the pre-treated cases.

#### 4 Discussion

OSF is a chronic progressive, precancerous condition of the oral cavity, characterized by fibrosis of the mucosal lining of the oral mucosa. The oral fibrosis often progresses into the submucosal regions and the underlying muscle, leading to deposition of dense fibrous bands and consequently restricts the opening of the mouth. The risk of cancer development in the upper aerodigestive tract is increased markedly in patients with OSF.<sup>28</sup> Collagen is the major structural component of the connective tissues, and its composition within each tissue needs to be maintained for proper tissue integrity. Although

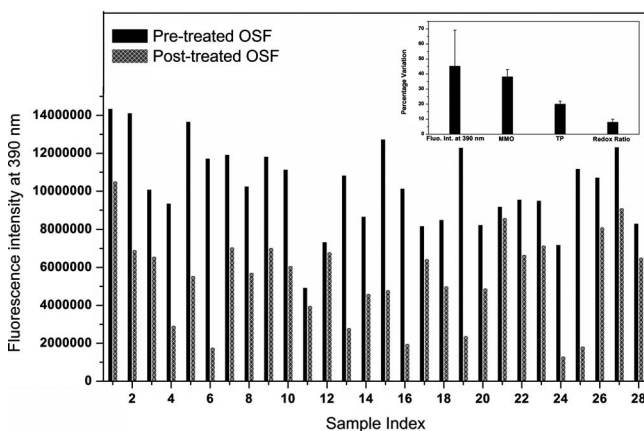


**Fig. 9** Individual fluorescence intensity of collagen at 390 nm for pre- and post-treated OSF patients. Inset shows the overall percentage variation of collagen emission, clinical evaluation (MMO and TP), and redox ratio.

the pathogenesis of OSF has been so far unclear, many data reported that OSF may be attributed to decreased secretion of collagenase and increased collagen production.<sup>29</sup> The current diagnostic procedure of OSF is to examine clinically the mouth opening, protrusion of tongue, burning sensation, and palpatory findings. As the prior clinical evaluations are visual inspections, the aforementioned procedures are indirect and do not provide information on the real condition of the patient's oral mucosa. This often requires a biopsy to confirm the clinical diagnosis.<sup>30</sup>

On the basis of these, there is much interest in developing a technique that does not require an invasive biopsy to diagnose oral lesions and that could also be used to monitor the effectiveness of chemopreventive and other therapeutic agents against oral neoplasia.

#### 4.1 *In Vivo* Fluorescence Spectroscopy

Although many reported that head and neck cancer can be discriminated from normal corresponding mucosa by fluorescence spectroscopy,<sup>8,31</sup> still the exact biochemical and structural changes responsible for altered spectral signatures at different sites in the oral cavity—as well as under different tissue transformation conditions, especially under different premalignant conditions—are not known. However, data reported that the structural protein, collagen, and the enzymes NADH and FAD are responsible for altered fluorescence when normal tissues are transformed into neoplastic. This is because it is unanimously considered that the aforementioned fluorophores play a key role in tissue structural integrity and cellular metabolic activities, respectively.<sup>32</sup> It is further reported that emission due to NADH from cancerous oral tissues is higher than that due to collagen, and vice versa for normal.<sup>12</sup> However, Chen et al.<sup>33</sup> reported that OSF mucosa at 330-nm excitation has very unique autofluorescence characteristics from that of other oral premalignant and malignant conditions. They reported that OSF mucosa had a significantly higher emission at 380 nm and lower emission at 460 nm than normal. Their study further revealed that there is a significant correlation between the spectral characteristics of OSF and clinical investigation by MMO.

Under these circumstances, we further attempted to study the *in vivo* autofluorescence characteristics of OSF patients to verify whether there is any possibility to discriminate OSF from normal, as well as monitor the effectiveness of drugs against OSF, and if there exists any statistical significance between them.

As was already mentioned, OSF is considered to be connected with collagen synthesis degradation and excess formation of collagen, *in vivo* fluorescence spectroscopic characterization was carried out at 330 nm. From Fig. 3 it is observed that the emission intensity at 390 nm from OSF is considerably higher than that of 465 nm. However, it is vice versa in the case of normal and post-treated cases. The reasons for the change in the spectral signatures between normal and OSF cases as well as between pre- and post-treated conditions may be considered as follows. The enhanced emission at 390 nm for OSF cases may be attributed to emission of collagen, indicating that there is an excess contribution of structural protein, collagen under OSF conditions. The emission at 465 nm is ascribed due to NADH.<sup>34</sup> These variations in the spectral

characteristics between normal oral mucosa and OSF cases are highly correlating with that reported by Chen et al. They reported that the increased collagen content in subepithelial connective tissue, and the probability of allowing more excitation energy by OSF mucosa than normal to penetrate into the subepithelial connective tissue, may be possible reasons for the enhanced fluorescence from OSF with respect to normal mucosa. Further, they reported that the OSF epithelium may contain a lesser amount of NADH than normal oral epithelium, and the fibrosis-induced reduction of blood vessels in the lamina propria might also reduce the metabolic rate of oral epithelial cells and hence lower the NADH content in the OSF. This result in OSF had significant lower emission intensity at 460 nm than that of normal cases.

Further, it is observed that the measured fluorescence spectra of post-treated cases resemble that of normal subjects. However, the overall emission intensity from normal is higher than that of post-treated OSF cases. OSF is considered to be an oral disease characterized by epithelial atrophy and progressive deposition of collagen in the lamina propria and submucosal of the oral mucosa. The given drug, hyaluronidase, when administered subcutaneously, increases the tissue permeability by depolymerizing hyaluronic acid, an essential component of the intercellular ground substance that determines the permeability of the tissues. It also exhibits spreading activity and breakdown of hyaluronic acid, lowering the viscosity of intercellular substances, thereby decreasing collagen formation.<sup>35</sup> Furthermore, it acts as a fibrinolytic agent, thereby a degrading of fibrotic bands. On the other hand, the drug dexamethasone sodium phosphate acts as an anti-inflammatory and immunosuppressant agent. It prevents fibrosis by decreasing fibroblastic proliferation and deposition of collagen. The combined effect of these drugs reduces the synthesis of collagen and/or regulating collagen synthesis, and therefore there is a decrease in fluorescence at 390 nm in post-treated cases.

Some investigators have extracted the intrinsic fluorescence spectra from *in vivo* fluorescence spectra in the cervix<sup>36</sup> and the oral cavity<sup>12</sup> with a mathematical model. Muller et al. found that in the oral cavity, the intrinsic fluorescence spectra could be composed of two spectral components, namely NADH and collagen, and that the NADH contribution increases, whereas the collagen contribution decreases as lesions become more malignant. Moreover, the loss of fluorescence of collagen at 390-nm intensity in oral lesions, as observed in both autofluorescence spectra and images, can be explained mostly by changes in stromal optical and morphologic properties. Lane et al.<sup>16</sup> reported that the loss of autofluorescence signal in images of oral precancerous and cancerous lesions is primarily due to the breakdown of the collagen matrix and increased hemoglobin absorption, and secondarily to epithelial factors such as increased epithelial scattering and thickness. In this context, it is worth noting that the spectral signature of malignant and other premalignant tissue is entirely different from that of OSF.

#### 4.2 Statistical Analysis

In this study, three different discriminant analyses were performed to find the sensitivity and specificity of the present technique to discriminate the different groups. The first dis-

criminant analysis  $D_1$  (the discrimination of OSF from normal) shows 100% specificity and 89.3% sensitivity with an overall accuracy of 94.6%. The discriminant analysis  $D_2$  discriminates post-treated from pretreated with 96.4% specificity and 89.3% sensitivity with an overall accuracy of 92.9%. The third discriminant analysis performed across the three groups, i.e., normal, pre-, and post-treated OSF cases. From the scatter plot (Fig. 6), it is well documented that both normal and post-treated cases have discriminant scores ( $D_3$ ) less than zero, whereas the pretreated cases show  $D_3$  values greater than zero. Note that discriminant analyses 1 and 2 resulted in a discriminant function involving ratio variables  $V_1$ ,  $V_4$ ,  $V_5$ ,  $V_7$ , and  $V_{11}$ , which correspond to the ratio variables  $I_{385}/I_{550}$ ,  $I_{385}/I_{468}$ ,  $I_{387}/I_{468}$ ,  $I_{385}/I_{355}$ , and  $I_{530}/I_{450}$  indicating that the key endogenous fluorophores such as collagen, NADH, and FAD correspond to the wavelengths responsible for the classification of normal from OSF as well as post-treated from pretreated cases.

#### 4.3 Reduction and Oxidation Ratio

Recently, it was well documented that neoplastic cells have an increased metabolic activity relative to normal cells; the native fluorescence characteristics of coenzymes NADH and FAD are also considered to study the metabolic rate of the cellular system and vascular oxygen supply.<sup>37</sup> Skala et al. reported that the steady- and excited-state characteristics of these metabolic coenzymes vary depending on the binding site and distribution. Furthermore, the redox ratio of this electron acceptor and donor fluorophores can also be considered to evaluate the histological state of tissue. In this context, the redox ratio of the cellular system is also used for chemotherapy drug monitoring.<sup>38</sup>

On the basis of these, the redox ratio values were also computed for normal subjects and OSF patients under both pre- and post-treated conditions. Although data reported that the redox ratio value usually decreases in neoplastic cells due to their increased metabolic activity, the same reason may not be considered for OSF, since OSF is primarily due to collagen metabolic disorders. This warranted further studies to understand the possible reasons of higher redox values for OSF compared to normal and post-treated cases. In spite of these, the redox ratio may also be considered a noninvasive complementary optical method to discriminate the OSF from normal as well as in the monitoring of the response of treatment.

#### 4.4 Clinical Evaluation

In the clinical evaluation of OSF, maximal mouth opening and tongue protrusion are conventionally used to monitor pre- and post-treated OSF patients. Maximal mouth opening is the interincisal distance as measured from the mesioincisal edge of the upper left central incisor tooth to the mesioincisal edge of the lower left central incisor tooth. The degree of tongue protrusion was recorded from the incisal edge of the lower teeth. A burning sensation is a preliminary record based on the patient's response. All these are based on the report from the patients and physical examinations only. Improvements in the treatment or impairment of oral diseases are considered by these factors.<sup>39</sup>

Table 1 shows the report of the clinical examination of MMO and TP of the patients. From Fig. 8 it is observed that

the values of MMO and TP are considerably increased due to treatment. MMO and TP values between pre- and post-treated OSF patients showed good statistical significance ( $p \cong 0.001$ ). This clearly indicates that there is a histological change due to treatment. The improvement in mouth opening and tongue protrusion as a result of treatment also correlates well with the native fluorescence characteristics.

Figure 9 indicates the absolute fluorescence intensity at 390 nm for both pre- and post-treated cases. From Fig. 9 it is observed that, except two cases, there is a considerable reduction in the fluorescence intensity after treatment with respect to pretreated cases. This clearly indicates that there is a considerable collagen reduction or collagen degradation due to treatment and the corresponding fluorescence change. The overall change (in percentage) due to the treatment for the measured intensity at 390 nm ( $I_{390}$ ) and redox values, along with MMO and TP, is shown in the inset. The inset clearly indicates that the change in intensity at 390 nm is highly comparable with that of MMO. This also clearly indicates that there is a change in the collagen content in tissue structure.

## 5 Conclusion

In conclusion, the present study reveals that the native fluorescence spectroscopic characterization of oral tissues could be extended to diagnose OSF cases, as well as used in the therapeutic prognosis of diseases. The results of spectroscopic analysis of oral tissues also correlate well with that of conventional clinical examinations and redox values. We hypothesize that the increase in fluorescence at 330-nm excitation is due to the up-regulation of collagen synthesis and down-regulation of collagenase production. However, further studies need to be carried out to prove that the level of collagen and collagenase is the direct cause of the altered spectral signature. Also, the reason for altered emission of NADH and FAD must be analyzed as well to understand the change in the photophysical characterization of fluorophores. Our pilot study can also be considered as a complementary method in the monitoring the treatment prognosis of OSF.

## Acknowledgments

This work was carried out using facilities funded by the Department of Science and Technology (DST), Government of India, grant number SP/S2/L-14/96. Author S. Sivabalan acknowledges the UGC for the award of JRF.

## References

1. M. Rahman, P. Chturvedi, A. M. Gillenwater, and R. Richards-Kortum, "Low-cost, multimodal, portable screening system for early detection of oral cancer," *J. Biomed. Opt.* **13**(3), 030502 (2008).
2. S. K. Mithani, W. K. Mydlarz, F. L. Grumbine, I. M. Smith, and J. A. Califano, "Molecular genetics of premalignant oral lesions," *Oral Dis.* **13**, 126–133 (2007).
3. V. K. Hazarey, D. M. Erlewad, K. A. Mundhe, and S. N. Ughade, "Oral submucous fibrosis: study of 1000 cases from central India," *J. Oral Pathol.* **36**(1), 12–17 (2007).
4. M. C. Chang, C. P. Chiang, C. L. Lin, J. J. Lee, L. J. Hahn, and J. H. Jeng, "Cell-mediated immunity and head and neck cancer: With special emphasis on betel quid chewing habit," *Oral Oncol.* **41**, 757–775 (2005).
5. S. M. Haider, A. T. Merchant, F. F. Fikree, and M. H. Rahbar, "Clinical and functional staging of oral submucous fibrosis," *Br. J. Oral Maxillofac Surg.* **38**, 12–15 (2000).
6. K. Yoshimura, U. B. Dissanayake, D. Nanayakkara, I. Kageyama, and K. Kobayashi, "Morphological changes in oral mucosae and their connective tissue cores regarding oral submucous fibrosis," **68**(3), 185–192 (2005).
7. M. C. Skala, G. M. Palmer, C. Zhu, Q. Liu, K. M. Vrotsos, C. L. Marshak-Stone, A. Gendron-Fitzpatrick, and N. Ramanujam, "Investigation of fiber-optic probe designs for optical spectroscopic diagnosis of epithelial pre-cancers," *Lasers Surg. Med.* **34**, 25–38 (2004).
8. D. R. Ingrams, J. K. Dhingra, K. Roy, D. F. Perrault Jr., I. D. Bottrill, S. Kabani, E. E. Rebeiz, M. M. Pankratov, S. M. Shapshay, R. Manoharan, I. Itzkan, and M. S. Feld, "Autofluorescence characteristics of oral mucosa," *Head Neck* **19**, 27–32 (1997).
9. A. Gillenwater, R. Jacob, R. Ganeshappa, B. Kemp, A. K. El-Naggar, J. Lynn Palmer, G. Clayman, M. Follen Mitchell, and R. Richards-Kortum, "Noninvasive diagnosis of oral neoplasia based on fluorescence spectroscopy and native tissue autofluorescence," *Arch. Otolaryngol. Head Neck Surg.* **124**(11), 1251–1258 (1998).
10. S. P. Schantz, V. Kolli, H. E. Savage, G. Yu, J. P. Shah, D. E. Harris, A. Katz, R. R. Alfano, and A. G. Huvos, "In vivo native cellular fluorescence and histological characteristics of head and neck cancer," *Clin. Cancer Res.* **4**(5), 1177–1182 (1998).
11. N. Subhash, J. R. Mallia, S. S. Thomas, A. Mathews, P. Sebastian, and J. Madhavan, "Oral cancer detection using diffuse reflectance spectral ratio R540/R575 of oxygenated hemoglobin bands," *J. Biomed. Opt.* **11**, 014018 (2006).
12. M. G. Muller, T. A. Valdez, I. Georgakoudi, V. Backman, C. Fuentes, S. Kabani, N. Laver, Z. Wang, C. W. Boone, R. R. Dasari, S. M. Shapshay, and M. S. Feld, "Spectroscopic detection and evaluation of morphologic and biochemical changes in early human oral carcinoma," *Cancer* **97**(7), 1681–1692 (2003).
13. S. K. Majumder and P. K. Gupta, "Synchronous luminescence spectroscopy for oral cancer diagnosis," *Lasers Life Sci.* **9**(3), 143–152 (2000).
14. C. Murali Krishna, N. B. Prathima, R. Malini, B. M. Vadhiraja, R. A. Bhatt, D. J. Hernandez, P. Kushtagi, M. S. Vidyasagar, and V. B. Kartha, "Raman spectroscopy studies for diagnosis of cancers in human uterine cervix," *Vib. Spectrosc.* **41**, 136–141 (2006).
15. E. Svistun, R. Alizadeh-Naderi, A. El-Naggar, R. Jacob, A. Gillenwater, and R. Richards-Kortum, "Vision enhancement system for detection of oral cavity neoplasia based on autofluorescence," *Head Neck* **26**, 205–215 (2004).
16. P. M. Lane, T. Gilhuly, P. Whitehead, H. Zeng, C. F. Poh, S. Ng, P. M. Williams, L. Zhang, M. P. Rosin, and C. E. MacAulay, "Simple device for the direct visualization of oral-cavity tissue fluorescence," *J. Biomed. Opt.* **11**, 024006 (2006).
17. R. J. Mallia, S. S. Thomas, A. Mathews, R. Kumar, P. Sebastian, J. Madhavan, and N. Subhash, "Laser-induced autofluorescence spectral ratio reference standard for early discrimination of oral cancer," *Cancer* **112**(7), 1503–1512 (2008).
18. R. R. Alfano, B. B. Das, J. Cleary, R. Prudente, and E. J. Celmer, "Light sheds light on cancer-distinguishing malignant tumors from benign tissue and tumors," *Bull. N. Y. Acad. Med.* **67**(2), 143–150 (1991).
19. S. Anderson-Engels, J. Johansson, K. Svanberg, and S. Svanberg, "Fluorescence imaging and point measurements of tissue: application to the demarcation of malignant tumors and atherosclerotic lesions from normal tissues," *Photochem. Photobiol.* **53**, 807–814 (1991).
20. N. Vengadesan, P. Aruna, and S. Ganesan, "Characterization of native fluorescence from DMBA-treated hamster cheek pouch buccal mucosa for measuring tissue transformation," *Br. J. Cancer* **77**(3), 391–395 (1998).
21. D. C. G. de Veld, M. Skurichina, M. J. H. Witjes, R. P. W. Duin, D. J. C. M. Sterenberg, W. M. Star, and J. L. N. Roodenburg, "Autofluorescence characteristics of healthy oral mucosa at different anatomical sites," *Lasers Surg. Med.* **32**, 367–376 (2003).
22. I. Pavlova, M. Williams, A. El-Naggar, R. Richards-Kortum, and A. Gillenwater, "Understanding the biological basis of autofluorescence imaging for oral cancer detection: high-resolution fluorescence microscopy in viable tissue," *Clin. Cancer Res.* **14**(8), 2396–2404 (2008).
23. M. C. Skala, K. M. Riching, D. K. Bird, A. Gendron-Fitzpatrick, J. Eickhoff, K. W. Eliceiri, P. J. Keely, and N. Ramanujam, "In vivo multiphoton fluorescence lifetime imaging of protein-bound and free nicotinamide adenine dinucleotide in normal and precancerous epithelia," *J. Biomed. Opt.* **12**(2), 024014 (2007).
24. M. C. Skala, K. M. Riching, A. Gendron-Fitzpatrick, J. Eickhoff, K.

- W. Eliceiri, J. G. White, and N. Ramanujam, "In vivo multiphoton microscopy of NADH and FAD redox states, fluorescence lifetimes, and cellular morphology in precancerous epithelia," *Proc. Natl. Acad. Sci. U.S.A.* **104**(49), 19494–19499 (2007).
25. C. Mujat, C. Greiner, A. Baldwin, J. M. Levitt, F. Tian, L. A. Stucenski, M. Hunter, Y. L. Kim, V. Backman, M. Feld, K. Munger, and I. Georgakoudi, "Endogenous optical biomarkers of normal and human papillomavirus immortalized epithelial cells," *Int. J. Cancer* **122**, 363–371 (2008).
  26. S. Madhuri, N. Vengadesan, P. Aruna, D. Koteeswaran, P. Venkatesan, and S. Ganesan, "Native fluorescence spectroscopy of blood plasma in the characterization of oral malignancy," *Photochem. Photobiol.* **78**(2), 197–204 (2003).
  27. N. Ramanujam, M. F. Mitchell, A. Mahadevan, S. Thomsen, A. Malpica, T. Wright, N. Atkinson, and R. R. Kortum, "Development of multivariate statistical algorithm to analyze human cervical tissue fluorescence spectra acquired *in vivo*," *Lasers Surg. Med.* **19**, 46–62 (1996).
  28. W. M. Tilakaratne, M. F. Klinikowski, Takashi Saku, T. J. Peters, and S. Warnakulasuriya, "Oral submucous fibrosis: review on aetiology and pathogenesis," *Oral Oncol.* **42**, 561–568 (2006).
  29. P. Rajalalitha and S. Vali, "Molecular pathogenesis of oral submucous fibrosis—a collagen metabolic disorder," *J. Oral Pathol. Med.* **34**, 321–328 (2005).
  30. C. K. Lee, M. T. Tsai, H. C. Lee, H. M. Chen, C. P. Chiang, Y. M. Wang, C. C. Yang, "Diagnosis of oral submucous fibrosis with optical coherence tomography," *J. Biomed. Opt.* **14**(5), 054008 (2009).
  31. D. L. Heintzelman, U. Utzinger, H. Fuchs, A. Zuluaga, K. Gossage, A. M. Gillenwater, R. Jacob, B. Kemp, and R. R. Richards-Kortum, "Optimal excitation wavelengths for *in vivo* detection of oral neoplasia using fluorescence spectroscopy," *Photochem. Photobiol.* **72**, 103–113 (2000).
  32. I. Pavlova, K. Sokolov, R. Drezek, A. Malpica, M. Follen, and R. Richards-Kortum, "Microanatomical and biochemical origins of normal and precancerous cervical autofluorescence using laser-scanning fluorescence confocal microscopy," *Photochem. Photobiol.* **77**, 550–555 (2003).
  33. H. M. Chen, C. Y. Wang, C. T. Chen, H. Yang, Y. S. Kuo, W. H. Lan, M. Y.-P. Kuo, and C. P. Chiang, "Auto-fluorescence spectra of oral submucous fibrosis," *J. Oral Pathol. Med.* **32**, 337–343 (2003).
  34. H. Schneckenburger, M. H. Gschwend, W. S. L. Strauss, R. Sailer, and R. Steiner, "Time-gated microscopic energy transfer measurements for probing mitochondrial metabolism," *Clin. Pharmacol. Ther.* **7**(1), 3–10 (1997).
  35. R. S. Satoskar, S. D. Bhandarkar, and S. S. Ainapure, *Pharmacology and Pharmacotherapeutics*, pp. 112–115, Popular Prakashan Publications, Mumbai (2005).
  36. I. Georgakoudi, B. C. Jacobson, M. G. Müller, E. E. Sheets, K. Badizadegan, D. L. Carr-Locke, C. P. Crum, C. W. Boone, R. R. Dasari, J. Van Dam, and M. S. Feld, "NADH and collagen as *in vivo* quantitative fluorescent biomarkers of epithelial precancerous changes," *Cancer Res.* **62**(3), 682–687 (2002).
  37. R. Drezek, C. Brookner, I. Pavlova, I. Boiko, A. Malpica, R. Lotan, M. Follen, and R. Richards-Kortum, "Autofluorescence microscopy of fresh cervical-tissue sections reveals alterations in tissue biochemistry with dysplasia," *Photochem. Photobiol.* **73**(6), 636–641 (2001).
  38. N. D. Kirkpatrick, C. Zou, M. A. Brewer, W. R. Brands, R. A. Drezek, and U. Utzinger, "Endogenous fluorescence spectroscopy of cell suspensions for chemopreventive drug monitoring," *Photochem. Photobiol.* **81**, 125–134 (2005).
  39. A. Kumar, A. Bagewadi, MDS, V. Keluskar, and M. Singh, "Efficacy of lycopene in the management of oral submucous fibrosis," *Oral Surg. Oral Med. Oral Pathol. Oral Radiol. Endod.* **103**(2), 207–213 (2007).